

Identification of a Cyanine-Dye Labeled Peptidic Ligand for Y₁R and Y₄R, Based upon the Neuropeptide Y C-Terminal Analogue, BVD-15

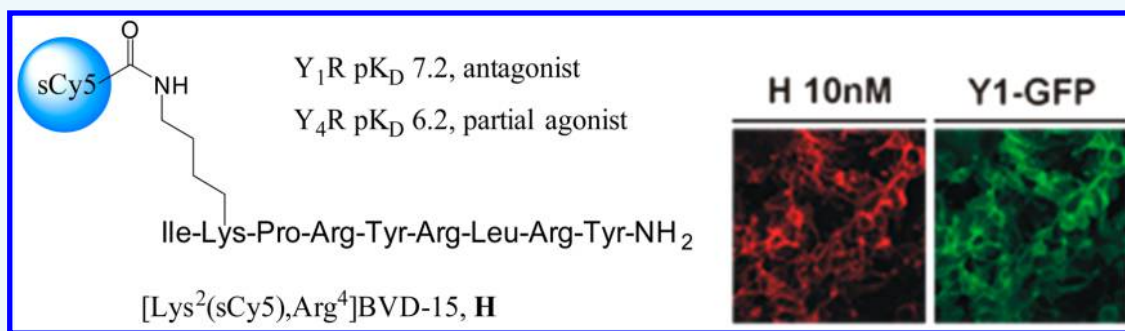
Mengjie Liu,[†] Rachel R. Richardson,[§] Simon J. Mountford,[†] Lei Zhang,[‡] Matheus H. Tempone,[§] Herbert Herzog,[‡] Nicholas D. Holliday,^{*,§} and Philip E. Thompson^{*,†}

[†]Medicinal Chemistry, Monash Institute of Pharmaceutical Sciences, Monash University, 381 Royal Parade, Parkville, VIC 3052, Australia

[‡]Neuroscience Division, Garvan Institute of Medical Research, St. Vincent's Hospital, Darlinghurst, NSW 2010, Australia

[§]Cell Signalling Research Group, School of Life Sciences, University of Nottingham, Queen's Medical Centre, Nottingham, NG7 2UH, United Kingdom

S Supporting Information



ABSTRACT: Traceable truncated Neuropeptide Y (NPY) analogues with Y₁ receptor (Y₁R) affinity and selectivity are highly desirable tools in studying receptor location, regulation, and biological functions. A range of fluorescently labeled analogues of a reported Y₁R/Y₄R preferring ligand BVD-15 have been prepared and evaluated using high content imaging techniques. One peptide, [Lys²(sCy5), Arg⁴]BVD-15, was characterized as an Y₁R antagonist with a pK_D of 7.2 measured by saturation analysis using fluorescent imaging. The peptide showed 8-fold lower affinity for Y₄R (pK_D = 6.2) and was a partial agonist at this receptor. The suitability of [Lys²(sCy5), Arg⁴]BVD-15 for Y₁R and Y₄R competition binding experiments was also demonstrated in intact cells. The nature of the label was shown to be critical with replacement of sCy5 by the more hydrophobic Cy5.5 resulting in a switch from Y₁R antagonist to Y₁R partial agonist.

INTRODUCTION

Neuropeptide Y (NPY) is a 36-amino-acid, C-terminal amidated polypeptide first isolated from porcine brain by Tatemoto's group in 1982.¹ It is a member of the NPY peptide family along with pancreatic polypeptide (PP, isolated in 1983)² and peptide YY (PYY, isolated in 1980),³ which both share a high degree of homology in amino acid sequence. The physiological functions of NPY are mediated by Y receptors, belonging to the rhodopsin-like G_i coupled G protein-coupled receptor (GPCR) family and four subtypes, Y₁R, Y₂R, Y₄R, and Y₅R have been identified in humans.^{4–6} Y₁R is expressed abundantly in both central and peripheral sympathetic nervous systems, and the NPY/Y₁R signaling cascade is implicated in various physiological responses, including regulation of feeding behavior,^{7,8} stimulation of ethanol intake,^{9,10} vasoconstriction,^{11,12} and initiation of anxiety and depression.^{13,14} In addition, breast carcinomas, including primary tumors and lymph node metastases, have also been found to overexpress Y₁R.¹⁵ This suggests that Y₁R may be responsible in tumor proliferation, apoptosis, metastasis and angiogenesis.¹⁶

With Y₁R being a potential drug target, traceable high affinity Y₁R ligands are highly desirable tools for studying the localization, regulation, and functions of this receptor. Lys⁴(sCy5)-NPY was shown to be an agonist of Y₁R, Y₂R, and Y₄R receptors, and of utility in the development of FACS-based functional assays of complex cell-based assay systems.¹⁷ Another approach has been to derive fluorescent or radio-labeled analogues of the Y₁R arginamide antagonist series (BIBP3226, BIBO3304),¹⁸ including pyridinium and cyanine based BIBP3226 derivatives suitable for fluorescent imaging.^{19,20} An alternative starting point has made use of smaller NPY derived peptide ligands, such as the competitive Y₁R antagonist/Y₄R agonist BVD-15 (or BW1911U90), a non-peptide modified from the NPY C-terminal fragment (Figure 1).²¹ This peptide has been amenable to conjugation with a variety of radiolabels and fluorophores. In particular, Guérin et

Received: July 12, 2016

Revised: August 8, 2016

Published: August 11, 2016

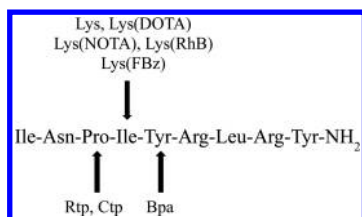


Figure 1. Amino acid sequence of BVD-15 scaffold and reported conjugated amino acid replacements. FBz = 4-fluorobenzoyl, Rtp = rhodamine B-triazolyl-proline, Ctp = coumarin-triazolyl-proline, Bpa = 4-benzoylphenylalanine.

al. showed that the Ile⁴ residue could be substituted by conjugated Lys to incorporate DOTA, NOTA or fluorine moieties,^{22,23} and we extended this result to include a rhodamine fluorophore.²⁴ No less notably, the Lys⁴ substitution itself resulted in increased affinity,²³ and other basic residues were also well tolerated.²⁴ This prompted us to examine such analogues with Pro³ as a point of conjugation and we have recently described propargyloxypyrrolidine containing Lys⁴- and Arg⁴-BVD-15 that could incorporate rhodamine B and 7-aminocoumarin fluorophores.²⁵ The tyrosine at the 5-position has been also shown to be capable of replacement with a conjugate group.²⁶

Noting that the position and nature of the conjugated group and its linkage could have a significant influence on the pharmacology of the resulting peptide, here we have examined the 2- and 4-position as the points of conjugation, and identified a number of potent novel fluorescently labeled Y₁R-targeting peptidic ligands. We have explored the utility of one of these and found it to be an excellent reagent for performing fluorescent imaging of recombinant cells transfected with Y₁R or Y₄R, allowing the development of receptor binding studies in intact living cells.

RESULTS AND DISCUSSION

Chemistry. We began by expanding our pool of conjugate precursors to include a variety of rhodamine B (RhB) conjugates (Figure 2), taking advantage of the capacity to

generate different linkers from a common, inexpensive precursor,²⁷ as well as two cyanine dyes (Figure 2) Cy5.5 and sulfo-Cy5 (sCy5). We extended the types of conjugates included at Lys⁴, but also encompassed substitutions at Asn². While a lysine residue at the 2-position had been shown to be detrimental to Y₁R activity,²³ the influence of subsequent conjugation had not been tested.

The synthesis of the conjugated BVD-15 analogues was achieved by one of three distinct methods. While all peptide backbones were prepared by adapting standard Fmoc-based solid phase peptide synthesis (SPPS) strategies, both solid and solution phase side-chain labeling were attempted. To facilitate chemoselective derivatization at the 2-position, the 4-position was substituted by an Arg residue, which retains high affinity for Y₁R receptors.²⁵

In the first instance, linear peptides were synthesized with N-terminal Fmoc protection and amide coupling in solution was achieved using carboxyl-functionalized fluorophores, followed by Fmoc-deprotection to yield the target peptides (analogues A, D, F, and H, using Method 1 in Scheme 1). In Method 2, selective ϵ -amine modification on solid phase was achieved by incorporating ϵ -Mtt-protected Lys as an orthogonal protection. The Mtt group was selectively cleaved off by treating with 25% HFIP and 5% TIPS, and then the Cy5.5 fluorophore was coupled as an N-succinimidyl ester. The N-terminal Fmoc group was removed by 20% piperidine prior to the final acidolytic cleavage, giving analogues E and G. In order to prepare analogues B and C where conjugates are linked by the 1,2,3-triazole group, Fmoc-Lys(azide)-OH was incorporated at the 4-position. Labeling was then achieved by solution phase CuAAC reaction using the alkyne-containing RhB-2 and RhB-3, in the presence of CuSO₄ and sodium ascorbate as the catalysts (Method 3).²⁵ The synthesized analogues with their analytical data are summarized in Table 1.

Pharmacological Analysis of NPY Analogues. We examined the functional properties of the BVD-15 analogues as antagonists of NPY-induced Y₁R engagement with β -arrestin2, a GPCR effector protein involved in G protein independent signaling and agonist induced receptor desensiti-

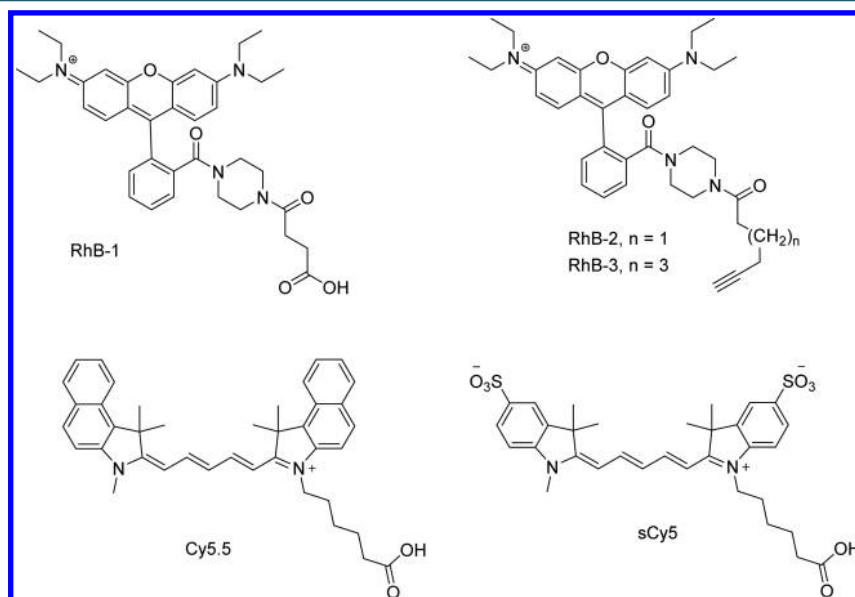
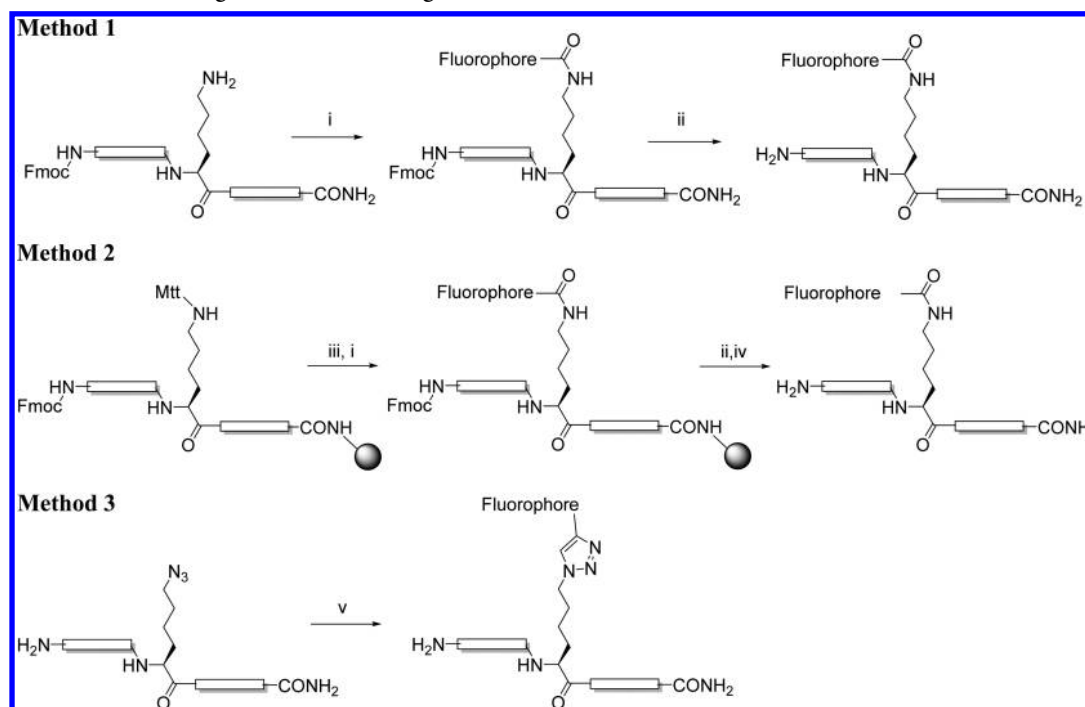


Figure 2. Fluorescent dye conjugates utilized in this study.

Scheme 1. Fluorescent Labeling of BVD-15 Analogues^a

^aReagents and Conditions: (i) fluorophore-COOH (1.2 equiv), PyClock (2 equiv), NMM (12 equiv), DMF, overnight (Note that for E and G, Cy5.5, was coupled as an N-succinimidyl ester); (ii) Piperidine (20%) in DMF, 5 min \times 2; (iii) HFIP (25%) and TIPS (5%) in DCM, 30 min; (iv) TFA-TIPS-DMB (92.5%:2.5%:5%), 3 h; (v) RhB-alkyne (2 equiv), CuSO₄ (0.5 equiv), THPTA (2.5 equiv), aminoguanidine (25 equiv), sodium ascorbate (25 equiv), DMSO 2% in potassium phosphate buffer (0.1 M, pH = 7.4), 1 h.

Table 1. Fluorescently Labeled BVD-15 Analogues and Their Analytical Data

code	sequence	MW (Calc.)	ESI-MS m/z^a	LC/MS ^b RT (min)	HPLC purity (%)
A	INPK(RhB-1) YRLRY-NH ₂	1815.2	605.9	10.24 ^c	93
B	INP(K-N ₃ -RhB-2) YRLRY-NH ₂	1839.3	613.9	13.42	99
C	INP(K-N ₃ -RhB-3) YRLRY-NH ₂	1867.3	623.3	13.58	99
D	IK(RhB-1) PRYRLRY-NH ₂	1857.3	620.1	13.09	99
E	INPK(Cy5.5) YRLRY-NH ₂	1786.5	596.6	14.12 ^d	94
F	INPK(sCy5) YRLRY-NH ₂	1859.3	621.2	12.72	98
G	IK(Cy5.5) PRYRLRY-NH ₂	1829.3	610.6	14.11 ^d	99
H	IK(sCy5) PRYRLRY-NH ₂	1901.3	635.4	12.06	98

^aESI-MS base peak corresponds to $[M+3H]^{3+}$. ^bHPLC retention time using a Phenomenex Luna C-8 column (100 Å, 3 μ m, 100 \times 2.00 mm). The gradient is composed of 100% H₂O (0.1% TFA) for 4 min, 0–60% acetonitrile in H₂O (0.1% TFA) over 10 min, and isocratic 60% acetonitrile in H₂O (0.1% TFA) for 1 min. Detection wavelength = 214 nm. ^cFor analogue A, the gradient is composed of 100% H₂O (0.1% TFA) for 4 min, 20–100% acetonitrile in H₂O (0.1% TFA) over 10 min, and isocratic 100% acetonitrile (0.1% TFA) for 1 min. ^dFor analogue E and G, the gradient is composed of 100% H₂O (0.1% TFA) for 4 min, 0–80% acetonitrile in H₂O (0.1% TFA) over 10 min, and isocratic 80% acetonitrile (0.1% TFA) for 1 min.

zation and internalization.²⁸ This assay gives a strong functional readout consistent with other second messenger assays, and the limited receptor reserve allows discrimination of agonist efficacy

via changes in R_{max} as compared to standard second messenger assays.^{20,21,28–30} Unlabeled $[Lys^4]BVD-15^{23,24}$ behaved as a competitive reversible antagonist of NPY stimulated responses, as indicated by Schild analysis (Figure 3A) with a pA_2 of 7.5, and all but one of the labeled ligands showed comparable high affinity antagonism. pK_b values were calculated from NPY concentration response curve shifts in the presence of a single antagonist concentration (100 or 300 nM; Figure S1), and ranged from 6.9 to 7.9 with the rhodamine-linked triazole compound B showing highest affinity (Table 2). Of the four cyanine labeled derivatives, three were antagonists (Table 2) with compound H $[Lys^2(sCy5), Arg^4]BVD-15$ showing highest affinity, and shared the surmountable antagonist characteristics of $[Lys^4]BVD-15$ (Figure 3B). Interestingly, substitution of the sCy5 fluorophore for Cy5.5 at the same 2-position led to compound G showing partial agonism in the Y₁R arrestin recruitment assay, with a pEC_{50} of 7.04 ± 0.19 and a maximal response of $52.8 \pm 4.8\%$ compared to that elicited by 1 μ M NPY ($n = 3$; Figure S2). In contrast, analogues E, F (both cyanine labeled at 4-position) and H showed no agonism at concentrations up to 1 μ M.

We screened the fluorescent BVD-15 analogues for their ability to specifically label 293TR cells stably expressing the GFP-tagged Y₁R. In plate-reader based imaging assays, RhB labeled derivatives (e.g., A, Figure 4) exhibited specific Y₁R receptor binding, predominantly localized to the plasma membrane that was inhibited by NPY and the nonpeptide Y₁R antagonist BIBO3304. Cy5.5 analogues (E, G) displayed significant nonspecific binding in addition to cellular labeling and were not pursued further. However, compound H displayed specific plasma membrane labeling of Y₁R-GFP cells at concentrations as low as 1 nM (Figure 5A), and specific

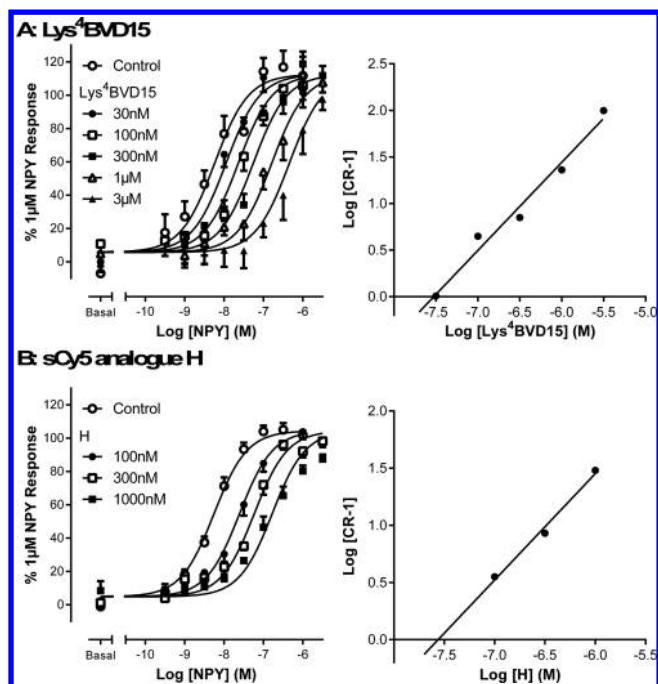


Figure 3. Surmountable antagonism of NPY stimulated Y_1R activation by unlabeled $[Lys^4]BVD15$ (Panel A) and sCy5-labeled derivative H (Panel B). Stably transfected HEK293 Y_1R - β -arrestin2 cells were pretreated for 30 min with the antagonist peptide at the indicated concentrations, prior to 1 h NPY stimulation. β -arrestin2 recruitment was quantified by high content imaging complementation assay as described in [Experimental Methods](#). Pooled data from 5 (A) or 4–7 experiments (B), globally fitted to obtain NPY pEC_{50} estimates, were used for Schild analysis in the right-hand panels. These derived pA_2 affinity estimates of 7.53 (analogue A) and 7.56 (analogue H) and respective slopes of 0.95 and 0.93, indicative of competitive reversible antagonism.

Table 2. Affinity Estimates for BVD-15 Analogues Derived from Functional Measurements or $[^{125}I]PYY$ Competition Binding

code	sequence	pK_b^a	pK_i (\pm SEM)
$[Lys^4]$ BVD-15 ²⁴	INPKYRLRY-NH ₂	7.5 ± 0.1	8.6 ± 0.1
A	INPK(RhB-1)YRLRY-NH ₂	7.6 ± 0.2	9.5 ± 0.2
B	INP(K-N ₃ -RhB-2)YRLRY-NH ₂	7.9 ± 0.2	9.6 ± 0.1
C	INP(K-N ₃ -RhB-3)YRLRY-NH ₂	7.6 ± 0.2	9.4 ± 0.1
D	IK(RhB-1)PRYRLRY-NH ₂	6.9 ± 0.4	9.2 ± 0.1
E	INPK(Cy5.5)YRLRY-NH ₂	7.3 ± 0.1	8.4 ± 0.2
F	INPK(sCy5)YRLRY-NH ₂	7.3 ± 0.1	N.D. ^c
G	IK(Cy5.5)PRYRLRY-NH ₂	agonist ^b	8.8 ± 0.3
H	IK(sCy5)PRYRLRY-NH ₂	7.5 ± 0.2	9.4 ± 0.1

^a pK_b estimates derived from pooled data using the Y_1R - β -arrestin2 recruitment assay presented in [Figure S1](#) ($n = 4$ or greater). For comparison, pK_i estimates ($n = 3$, except compound B $n = 2$) are derived from $[^{125}I]PYY$ binding studies in Y_1R -GFP membranes, performed under low sodium conditions in the absence of guanine nucleotides. ^b $pEC_{50} = 7.0 \pm 0.2$, partial agonist ([Figure S2](#)). ^cN.D. = not determined

binding was fully inhibited by unlabeled competitors such as NPY or BIBO3304.

Peptide H was therefore chosen to develop a plate-reader imaging based Y_1R binding assay, using living whole cells.

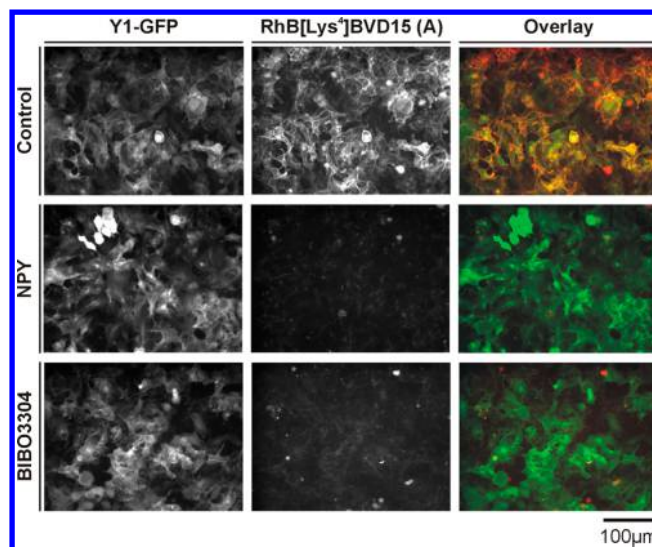


Figure 4. Cellular labeling of Y_1R -GFP by $[Lys^4(RhB)]BVD-15$ (A). 293TR Y_1R -GFP cells were incubated for 30 min at 37 °C with 10 nM A in the absence (control) or presence of 100 nM NPY or 100 nM BIBO3304. Representative IX Micro images (from one of three experiments) of GFP (left) or RhB fluorescence (center) are indicated, demonstrating extensive cell surface labeling using ligand A and colocalization with the GFP-tagged Y_1R .

Peptide H displayed fluorescence consistent with the sCy5 labeling, with excitation and emission maxima at 653 and 667 nm, respectively, and a relative quantum yield of 127% compared to sCy5-NHS alone ([SI Figure 4](#)). Based on optimized incubation conditions of 30 min at 37 °C, saturation analysis demonstrated one site binding and derived a Y_1R pK_D for H of 7.16 ± 0.06 ($n = 4$) ([Figure 5B](#)), an estimate of affinity that was not significantly different from the pK_i derived by functional analysis ([Figure 3](#)). Furthermore, initial BIBO3304 competition data compared a family of curves at different H concentrations (1, 10, and 100 nM), yielding BIBO3304 pIC_{50} values of 9.06 ± 0.07 , 8.69 ± 0.07 , and 8.31 ± 0.07 , respectively ($n = 4$, [Figure 5B](#)). The proportionate shift in competing ligand IC_{50} was consistent with equilibrium conditions and the Cheng-Prusoff relationship. Additional affinity estimates for BIBO3304 ($pK_i = 8.9$) and H ($pK_i = 7.3$) determined by this method were consistent with our other whole cell data.

Peptide H was employed in the study of a range of known Y receptor agonists, antagonists, as well as a series of analogues prepared in related studies ([Table 3](#)).^{29,31} The expected Y_1 -like pharmacology in the competition assay was observed for agonist peptides ([Figure 5D](#); NPY = $[Leu31, Pro34]NPY \geq PYY > PYY3-36 = PP$), as previously described for many Y_1 receptor systems,³² and also antagonists, such as the dimeric peptide 1229U91.²⁹ The order of affinity based on pK_i values from these experiments was consistent with $[^{125}I]PYY$ binding assays for representative ligands performed in Y_1R -GFP cell membranes (and previously described data from Y_2Y_4 receptor knockout mice).²⁹ For the nonpeptide antagonist BIBO3304 there was good correspondence between affinities measured in these formats, and also functional measurements previously reported.²⁸ For the peptide ligands the actual pK_i values for the whole cell assays were consistently lower than for membrane based assays ([Table 4](#)). The reason for this discrepancy is not obvious, but note that there is a closer correlation between the competition binding (pK_i) and the functional antagonism in the

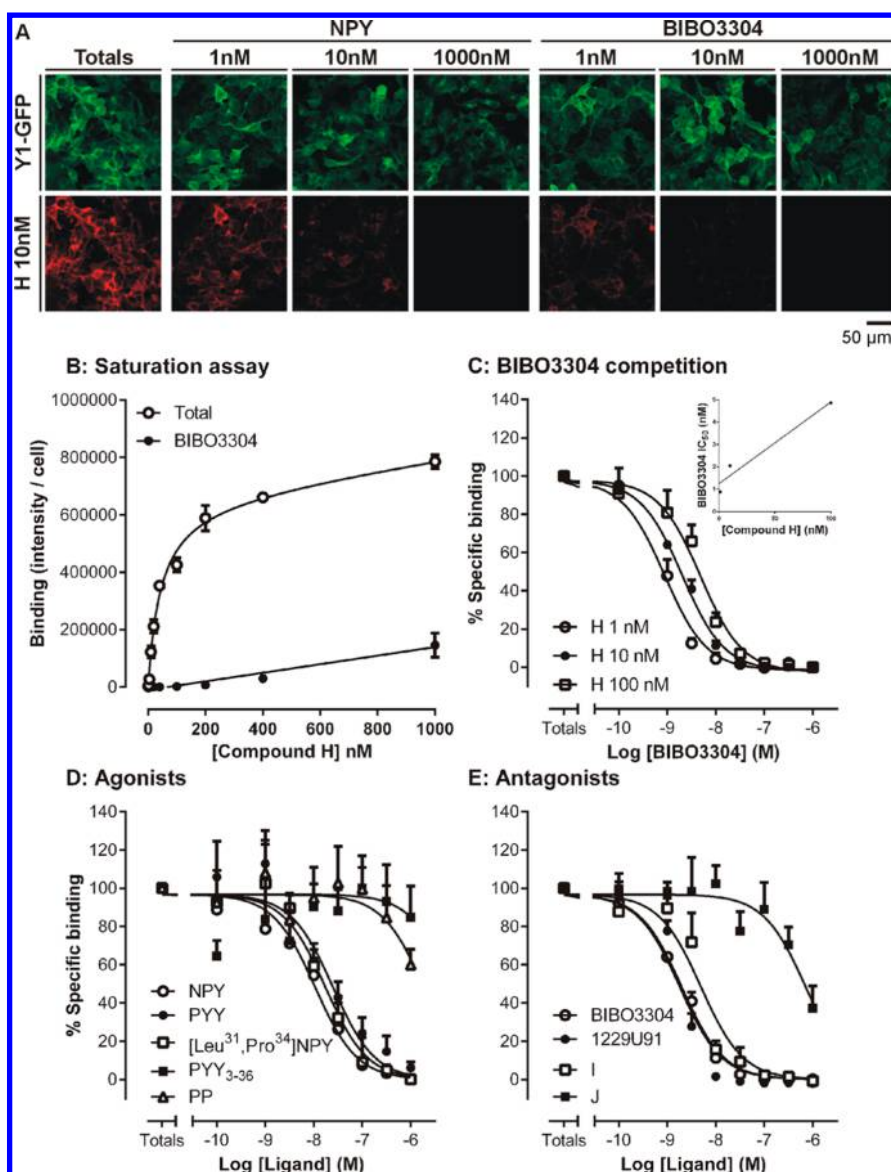


Figure 5. Y_1R binding assays using sCy5 labeled analogue **H**. Images from the IX Ultra platereader (Panel A, 400×400 pixels from original 1000×1000 acquisition) show binding of 10 nM **H** (red channel) to live 293TR Y_1R -GFP cells in the absence or presence of different NPY or BIBO3304 concentrations (30 min, with Y_1R -GFP images (green) also presented for comparison). Saturation analysis (Panel B) was performed in the absence (total) or presence of $1 \mu\text{M}$ BIBO3304 (example experiment representative of 4). Pooled competition binding data (Panels C–E, at least 3 experiments) were derived from granularity analysis of the ligand images, normalized to total specific binding (100%). In C, BIBO3304 competition curves were performed at three **H** concentrations; the plot of the BIBO3304 IC_{50} versus ligand concentration (inset) provides additional K_i affinity estimates for both BIBO3304 and **H** quoted in text (see [Experimental Methods](#)). pK_i estimates were also obtained for a range of agonist peptides (Panel D) and antagonists (Panel E), as indicated in Table 4.

whole cell system. The difference may be due to the buffer conditions in routine Y receptor membrane binding assays (low sodium and absence of guanine nucleotides) that are designed to promote the high affinity ternary receptor complex, and maximize radiolabeled agonist peptide binding.³³ The non-physiological buffer cation concentrations might also directly affect peptide ligand binding to the receptor. Thus, one of the important advantages of our measurements using fluorescent antagonist binding to whole cells, in physiological buffer, is that the affinities obtained should closely correspond to observations from functional data, particularly for agonists. Indeed, the estimates of agonist affinity by this route (Figure 5D) do closely correspond with their potencies in Y_1R -arrestin recruitment assay previously reported,²⁸ as anticipated for a response with

limited receptor reserve.³³ We also assayed compounds for which we had membrane competition binding data spanning a range of affinities, including analogues of 1229U91, **I** and **J** (Figure 5E; Table 3)²⁹ and some unlabeled BVD-15 analogues **K**–**N** (Table 3) and found the same trends (Table 4, Figure S3).

Compound **H** displayed moderate affinity for Y_4R (Figure 6), with saturation binding assays yielding a pK_D for **H** of 6.26 ± 0.11 ($n = 4$), 8-fold lower than for Y_1R . It did not bind cells expressing Y_2R or Y_5R (data not shown) at up to $1 \mu\text{M}$, as might be predicted from the reported selectivity profile for BVD-15.³⁵ In contrast to its actions at the Y_1R , **H** was a Y_4R partial agonist, a property shared by BVD-15, in the β -arrestin2 recruitment assay (Figure 6; $pEC_{50} = 7.10 \pm 0.19$, $1 \mu\text{M}$

Table 3. Analytical Data of Dimeric 1229U91 Analogues and Other Unlabeled BVD-15 Analogues

code	sequence	MW (Calc.)	ESI-MS m/z	LC/MS RT. (min) ^c	HPLC purity (%)
I	Bis(Lys ⁴) 1229U91 ²⁹	2436.9	851.6 ^a	11.16	98
J	Bis(des-Ile ¹) 1229U91 ²⁹	2126.4	748.1 ^a	11.00	99
K	FBz- INPKYRLRY- NH ₂	1343.6	672.8 ^b	12.30	97
L	INPOYRLRY- NH ₂ ²⁴	1207.4	604.7 ^b	10.55	98
M	FBz- INPRF*RLRY- NH ₂	1506.7	754.2 ^b	12.93	99
N	INPRF*RLRY- NH ₂	1384.6	693.2 ^b	11.51	98

^aESI-MS base peak corresponds to $[M+TFA+3H]^{3+}$. Note that $[M+3H]^{3+}$ peaks were observed at lower intensity. ^bESI-MS base peak corresponds to $[M+2H]^{2+}$. ^cHPLC retention time using a Phenomenex Luna C-8 column (100 Å, 3 μm, 100 × 2.00 mm). The gradient is composed of 100% H₂O (0.1% TFA) for 4 min, 0–60% acetonitrile in H₂O (0.1% TFA) over 10 min, and isocratic 60% acetonitrile in H₂O (0.1% TFA) for 1 min. Detection wavelength = 214 nm. FBz = 4-fluorobenzoyl, O = ornithine, F* = Phe(4-CH₂NH-FBz).

response $59.0 \pm 3.6\%$, 100 nM PP, $n = 6$); other cyanine BVD-15 analogues E–G displayed limited Y₄R agonism at the highest concentration tested (1 μM). At 100 nM, H selectively labeled 293TR cells expressing Y₄R-GFP (Figure 6A), enabling competition binding studies to derive pK_i estimates for human PP, 1229U91, and its analogues I and J (Figure 6C; Table 4). As previously discussed, these estimates were lower than those previously reported for [¹²⁵I]PP agonist binding studies in Y₄R containing membranes.³⁴ However, the estimates of PP and 1229U91 affinity in whole cells by this route closely corresponded with their potencies in the arrestin recruitment assay (PP pEC₅₀ = 8.77 ± 0.07 , $n = 5$; 1229U91 weak partial agonist pEC₅₀ = 7.43 ± 0.41 , $n = 4$; Figure 6D). Comparisons of Y₁R/Y₄R binding affinities of 1229U91 analogues demonstrated that I had equivalent Y₁R/Y₄R selectivity as 1229U91 (16–30-fold selective for Y₁R), while removal of the terminal Ile residues in J reversed the selectivity profile between these

subtypes (approximately 8-fold higher affinity for Y₄R over Y₁R).

In summary, our studies of fluorescent labeling of the BVD-15 scaffold has allowed us to identify some new features of the peptides' structure–activity relationships. First, we confirmed the general tolerance for modification at the 4-position, with retention of antagonistic activity at levels similar to the parent peptide in the presence of rhodamine derivatives and cyanine dyes. Second, we showed for the first time that the Asn residue at 2-position, in combination with introduction of an Arg at 4-position, yields peptides with retained affinity. However, while the sulfated Cy5 (sCy5) ligand is an antagonist, the more hydrophobic Cy5.5 label has agonist properties. This is significant as only one other example of a truncated NPY analogue has been shown to be an agonist.²⁶ We have also shown that analogue H is an excellent ligand for performing receptor binding studies at Y₁R in intact cells using high content imaging, with low levels of nonspecific binding. Finally, we also show that analogue H has Y₄R agonism, albeit at a lower level of affinity compared to Y₁R binding. Thus, analogue H is also a suitable ligand for conducting competition binding and functional assays against Y₄R and has been applied recently in structure–activity studies of the dimeric Y₄ agonist, BVD-74D.^{36,37} The ready synthesis of this fluorescent ligand and its favorable properties will be of great utility in the development of new ligands for these two important receptors.

EXPERIMENTAL METHODS

Material. N^α-Fmoc protected amino acids were purchased from Auspep, Chemimpex and Mimotopes. Rink amide resin (0.53 mequiv/g, 100–200 mesh), HCTU and PyClock were obtained from Chemimpex. TFA, TIPS, DMB, HFIP, DIPEA, piperidine, CuSO₄, aminoguanidine, sodium ascorbate, and DMSO were purchased from Sigma-Aldrich. All solvents were obtained from Merck. Cyanine dyes were purchased from Lumiprobe and W&J PharmaChem. THPTA was a gift from Dr Bim Graham's group (Monash Institute of Pharmaceutical Sciences, Monash University). The Rhodamine B derivatives were prepared in-house from the commercially available product (Sigma-Aldrich), according to Nguyen and Francis.²⁷ All solvents were of analytical grade, and all chemicals were used without further purification.

Table 4. Competition Binding Assays at Y₁R and Y₄R Using Compound H as a Competing Ligand, In Comparison to Radioligand Binding Data

peptide	Y ₁ R (pK _i) ^a live cell imaging (H)	Y ₁ R (pK _i) [¹²⁵ I]PYY membranes	Y ₄ R (pK _i) ^a live cell imaging (H)	Y ₄ R (pK _i) [¹²⁵ I]PP membranes
NPY	7.95 ± 0.12	9.75 ± 0.16	-	-
PYY	7.67 ± 0.10	9.50 ± 0.23	-	-
Leu ³¹ , Pro ³⁴ -NPY	7.82 ± 0.11	-	-	-
PYY(3–36)	<6.0	-	-	-
PP	<6.0	-	8.69 ± 0.11	10.1 ± 0.21 ³⁴
BIBO3304	8.76 ± 0.04	9.25 ± 0.11	-	-
1229U91	8.80 ± 0.07	9.90 ± 0.06	7.21 ± 0.10	9.6 ± 0.11 ³⁴
I	8.35 ± 0.12	10.18 ± 0.12	7.20 ± 0.10	-
J	6.03 ± 0.59	8.91 ± 0.08	6.91 ± 0.11	-
K	6.48 ± 0.17	9.10 ± 0.08	-	-
L	7.69 ± 0.09	9.73 ± 0.01	-	-
M	6.23 ± 0.11	8.62 ± 0.19	-	-
N	7.59 ± 0.10	9.74 ± 0.08	-	-

^apK_i estimates from $n = 3–4$ whole cell competition binding (H) in Y₁R-GFP or Y₄R-GFP cells, using the Cheng-Prusoff correction based on H pK_D derived from saturation analysis in imaging studies. pK_i estimates derived from [¹²⁵I]PYY binding to 293TR Y₁R-GFP membranes ($n = 2–6$).

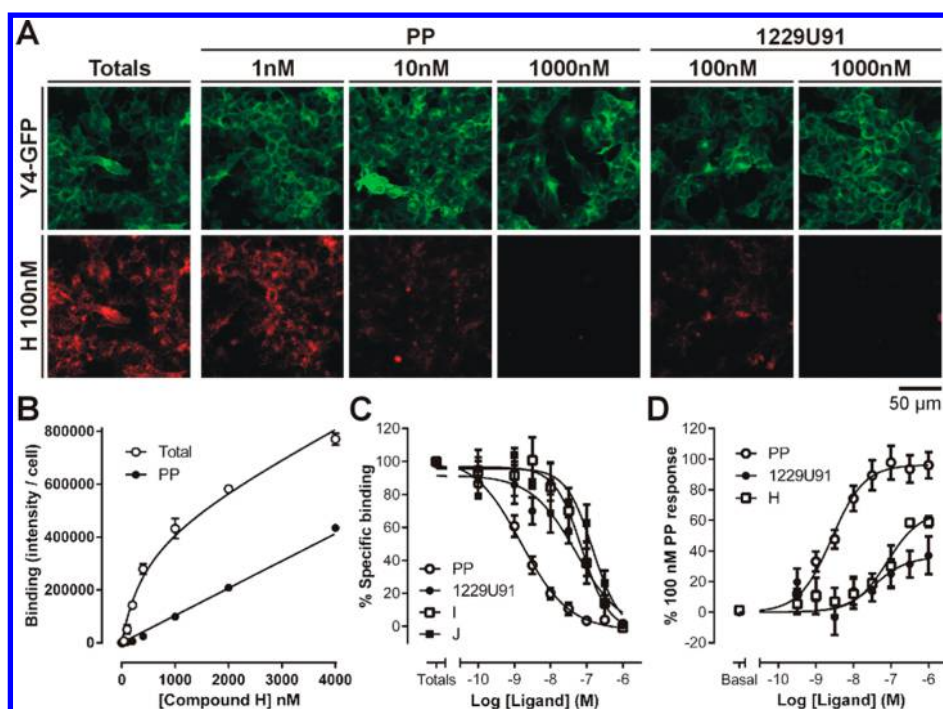


Figure 6. [Lys²(sCy5), Arg⁴]BVD-15 (H) is also a Y₄R fluorescent ligand. Panel A illustrates representative images of 100 nM H binding (red) to 293TR Y₄R-GFP cells (green) in the absence or presence of the endogenous peptide PP or 1229U91. Quantification of these data obtained saturation data for H (pK_D 6.26), in which nonspecific binding was assessed in the presence of 1 μ M PP (Panel B, experiment representative of 4), and competition curves in Panel C (pooled from 4 to 7 experiments), from which the pK_i estimates in Table 4 were determined. In the Y₄R- β -arrestin2 recruitment assay (Panel D), H was a partial agonist compared to PP, but of higher relative efficacy than 1229U91 (pooled data 4–10 experiments).

Molecular mass of peptides was determined by ESI-MS using a Shimadzu LCMS2020 instrument, incorporating a Phenomenex Luna C-8 column (100 Å, 3 μ m, 100 \times 2.00 mm). Detection wavelength was set at 214 nm. This system used 0.05% TFA in Milli-Q water as the aqueous buffer, and 0.05% TFA in acetonitrile as the organic buffer. The eluting profile was a linear gradient of 0–60% acetonitrile in water over 10 min at 0.2 mL/min.

Crude peptides were purified on a Phenomenex Luna C-8 column (100 Å, 10 μ m, 250 \times 21.2 mm) utilizing a Waters 600 semipreparative RP-HPLC that incorporates a Waters 486 UV detector. Detection wavelength was set at 230 nm. This system used 0.1% TFA in Milli-Q water as the aqueous buffer, and 0.1% TFA in acetonitrile as the organic buffer. The eluting profile was a linear gradient of 0–80% acetonitrile in water over 60 min at 10 mL/min.

Peptide Synthesis. General Synthesis. Linear peptides (0.1 mmol scale) were synthesized on Rink amide resin using a 3-channel serial automated peptide synthesizer (“PS3”, Protein Technologies Inc.), which adopted standard Fmoc-based solid-phase synthesis strategy. Fmoc deprotection was performed by piperidine (20% v/v) in DMF for 2 \times 5 min. Fmoc protected amino acids (3 equiv) were coupled using DMF as solvent, and DIPEA in DMF (7% v/v) with HCTU (3 equiv) as the activating agent for 50 min.

Protected peptidyl-resins were cleaved by treating with a cocktail (5 mL) composed of TFA-TIPS-DMB (92.5%:2.5%:5%) for 3 h. The cleavage mixture was then filtered, concentrated by stream of N₂, precipitated in cold Et₂O, and centrifuged at 3000 rpm for 5 min. The crude product was dissolved in water–acetonitrile mixture (50%:50%) and lyophilized.

Labeling Methods. Method 1. The N^α-Fmoc protected linear peptide dissolved in DMF (0.6 mL) was treated with carboxyl-functionalized fluorophore of interest (1.2 equiv), PyClock (2 equiv), and NMM (12 equiv) overnight. After DMF was removed in vacuo, the product was washed by TFA (1 mL), precipitated by cold Et₂O, and centrifuged at 3000 rpm for 5 min. The N^α-Fmoc group was then removed by piperidine (20%) in DMF (5 mL) for 30 min and the reagents were evaporated in vacuo. The product was redissolved in water–acetonitrile (50%:50%) and lyophilized.

Method 2. The protected peptidyl-resin containing a Lys(Mtt) residue was treated with HFIP (25%) and TIPS (5%) in DCM (5 mL) for 30 min to selectively remove the Mtt group. Cy5.5 (as an N-succinimidyl ester) was conjugated by treating overnight in an alkaline condition created by DIPEA (10 equiv).

Method 3. Linear peptide containing a Lys(azide) residue (15 mg) was labeled by treating with a mixture of RhB-alkyne (2 equiv), CuSO₄ (0.5 equiv), THPTA (2.5 equiv), sodium ascorbate (25 equiv), and aminoguanidine (25 equiv) in a potassium phosphate buffer containing 2% DMSO, where the final concentration of linear peptide was 0.2 mM. The mixture was stirred for 1 h and lyophilized.

Peptides were purified by RP-HPLC as described above. The purity of all peptides are \geq 93% according to the HPLC chromatographs produced by the ESI-MS method described above, and MS data corresponded to the expected m/z values. Additional details are provided in Table 1, Table 3, and Supporting Information.

Cell Culture. HEK293T and 293TR cells (Invitrogen) were cultured in Dulbecco’s modified Eagle’s medium (DMEM, Sigma-Aldrich) supplemented with 10% fetal bovine serum,

293TR cell lines inducibly expressing Y₁R or Y₄R tagged with C-terminal GFP, and dual HEK293 cells coexpressing Y receptor-Yc and β -arrestin2-Yn (where Yc and Yn are complementary fragments of YFP) are as previously reported.^{28,38}

[¹²⁵I]PYY Competition Binding Studies in Membranes.

Competition binding assays were carried out as described previously.^{28,38} Using membranes from the 293TR Y₁R-GFP cells, competition binding assays were performed for 90 min at 21 °C in buffer (25 mM HEPES, 2.5 mM CaCl₂, 1.0 mM MgCl₂, 0.1% bovine serum albumin, 0.1 mg/mL bacitracin; pH = 7.4), increasing concentrations of unlabeled ligands (10⁻¹² M to 10⁻⁶ M, duplicate) and [¹²⁵I]PYY (15 pM). Nonspecific binding in these experiments comprised less than 5% of total counts, and was subtracted from the data.

In both sets of data, IC₅₀ values were calculated from displacement curves (repeated 2–3 times for each peptide, fitted using nonlinear least-squares regression in GraphPad Prism v 6 (GraphPad software, San Diego CA, U.S.A.). They were converted to pK_i estimates using the Cheng-Prusoff relationship

$$K_i = \frac{IC_{50}}{1 + [RL]/K_{RL}}$$

where [RL] and K_{RL} represent the concentration and equilibrium dissociation constant of [¹²⁵I]PYY, respectively.

Y Receptor- β -Arrestin Recruitment Assays. Bimolecular fluorescence complementation (BiFC) based detection of Y receptor- β -arrestin2 association was performed as described previously.^{28,38} The Y receptor arrestin BiFC cell lines were seeded at 40 000 cells/well onto poly(D-lysine)-coated Greiner 655090 imaging plates, and experiments performed 24 h later. Stimulation with human NPY (Y₁R) or PP (Y₄R; Bachem, St. Helens, U.K.), or other ligands was performed in HEPES-buffered saline solution (HBSS) including 0.1% BSA (10⁻¹⁰ M–10⁻⁶ M) for 60 min at 37 °C, with antagonist preincubations (30 min, 37 °C) if required. Incubations were terminated by fixation with 3% paraformaldehyde in phosphate buffered saline (PBS, 10 min at 21 °C), the cells were washed once with PBS and the cell nuclei were stained for 15 min with H333342 (2 μ g/mL in PBS, Sigma). H333342 was then removed by a final PBS wash. Images (4 central sites/well) were acquired automatically on the IX Ultra confocal plate reader, using 405 nm/488 nm laser lines for H333342 and complemented YFP excitation, respectively.

A granularity algorithm (MetaXpress 5.3) identified internal fluorescent compartments within these images of at least 3 μ m diameter (range set to 3–12 μ m), on the basis of granule intensity thresholds set with reference to the vehicle or positive plate controls (e.g., 1 μ M NPY). The response for each data point (duplicate data) was quantified as mean granule average intensity/cell, normalized to the reference agonist response. Concentration response curves were fitted to the pooled data by nonlinear least-squares regression (GraphPad Prism), yielding estimates of agonist potency as pEC₅₀ and maximum response (R_{max}). Where appropriate, the Gaddum equation was used to calculate an estimate of antagonist affinity:

$$pK_b = \log[CR - 1] - \log[B]$$

where CR is the concentration ratio (NPY EC₅₀ in the presence of antagonist/control NPY EC₅₀), and [B] is the antagonist concentration used. To assess NPY concentration response

curves in the absence and presence of multiple antagonist concentrations ([Lys⁴]BVD-15 or compound H), Schild analysis was performed by global fitting of the curve families in GraphPad Prism; the Schild plot of log[CR - 1] versus log[B] illustrated the antagonist affinity estimate (pA₂) as the X-intercept of the fitted line.

Y Receptor Saturation and Competition Fluorescent Ligand Binding Assays.

293TR Y₁R-GFP or Y₄R-GFP cells were seeded at 20 000 cells/well in poly(D-lysine) coated 96-well Greiner 655090 imaging plates, treated as required with 1 μ g/mL tetracycline for 18–21 h and then used in experiments at confluence. Incubations were performed in HBSS/0.1% BSA, the permeable nuclear dye H333342 (2 μ g/mL, Sigma), and competitor ligands as appropriate (10⁻¹⁰ M to 10⁻⁵ M) for 2 min, prior to the addition of fluorescent ligand at the concentration indicated. In saturation studies, nonspecific binding was assessed in the presence of 1 μ M BIBO3304 (Y₁R) or PP (Y₄R). After 30 min at 37 °C the media was replaced with HBSS/0.1% BSA and plates were immediately imaged (2 sites/well). For cyanine analogues (e.g., H) an IX Ultra confocal plate reader (Molecular Devices, Sunnyvale CA, U.S.A.) used laser excitation/emission filter settings appropriate for H333342 (DAPI), Y receptor-GFP (FITC), and fluorescent ligand (Cy5). For rhodamine B derivatives an IX Micro epifluorescence plate reader (Molecular Devices) acquired the images using the TRITC excitation/emission filter set.

For fluorescent ligand binding using H, bound ligand fluorescence was quantified by granularity analysis (2–3- μ m-diameter granules; MetaXpress 5.3, Molecular Devices). Competition data were normalized to positive (totals 100%) and negative (0%, in the presence of either 1 μ M NPY or 100 nM PP as appropriate) controls. For saturation studies, total and nonspecific binding data were globally fitted using a one site binding model whereby

$$\text{Total binding} = B_{\max} \cdot \frac{[FL]}{[FL] + K_D} + NS \times [FL]$$

$$\text{Nonspecific binding} = NS \times [FL]$$

[FL] is the fluorescent ligand concentration, B_{max} represents the maximum specific binding, NS is the gradient of the nonspecific binding relationship, and K_D is the equilibrium dissociation constant for compound H.

pIC₅₀ values for unlabeled ligands were then determined from the pooled data using GraphPad Prism, and converted to pK_i using the Cheng-Prusoff relationship described above and the fluorescent ligand K_D estimated from saturation data. In competition experiments in which compound H concentration [FL] in the assay was varied, the plot of BIBO3304 IC₅₀ versus [FL] was fitted by linear regression using the relationship derived from the Cheng-Prusoff equation

$$IC_{50} = \frac{K_i}{K_D} \times [FL] + K_i$$

The y intercept for this fit derives an estimate of K_i for the competing ligand, BIBO3304, and the slope (K_i/K_D) also yields a further measurement of affinity of the fluorescent ligand H (K_D).

■ ASSOCIATED CONTENT

Supporting Information

The Supporting Information is available free of charge on the ACS Publications website at DOI: 10.1021/acs.bioconjchem.6b00376.

Detailed synthesis procedures as well as additional supplementary figures showing dose–response curves for Y₁R binding by peptides, fluorescence excitation/emission spectra for compound H, and HPLC profiles for synthesized peptides (PDF)

■ AUTHOR INFORMATION

Corresponding Authors

*E-mail: nicholas.holliday@nottingham.ac.uk, Tel: +44 115 82 30084, Fax: +44 115 82 30081.

*E-mail: philip.thompson@monash.edu, Tel: +61 3 99039672, Fax: +61 3 99039582.

Notes

The authors declare no competing financial interest.

■ ACKNOWLEDGMENTS

This work was supported by CRC for Biomedical Imaging Development (CRC-BID), Australia. M.L. was supported by an Australian Postgraduate Award scholarship. RRR was supported by the Nottingham-Monash PhD program.

■ ABBREVIATIONS

DCM, dichloromethane; DIPEA, *N,N*-diisopropylethylamine; DMB, 1,3-dimethoxybenzene; DMF, *N,N*-dimethylformamide; HCTU, *O*-(1*H*-6-chlorobenzotriazol-1-yl)-*N,N,N',N'*-tetramethyluronium hexafluorophosphate; HFIP, hexafluoroisopropanol; NMM, *N*-methylmorpholine; RhB, Rhodamine B; TFA, trifluoroacetic acid; THPTA, tris(3-hydroxypropyltriazolylmethyl)amine; TIPS, triisopropylsilane

■ REFERENCES

- (1) Tatemoto, K. (1982) Neuropeptide Y: Complete amino acid sequence of the brain peptide. *Proc. Natl. Acad. Sci. U. S. A.* 79, 5485–5489.
- (2) Hoffmann, J. A., and Chance, R. E. (1983) Crystallization of bovine pancreatic polypeptide. *Biochem. Biophys. Res. Commun.* 116, 830–835.
- (3) Tatemoto, K., and Mutt, V. (1980) Isolation of two novel candidate hormones using a chemical method for finding naturally occurring polypeptides. *Nature* 285, 417–418.
- (4) Blomqvist, A. G., and Herzog, H. (1997) Y-receptor subtypes - how many more? *Trends Neurosci.* 20, 294–298.
- (5) Bromée, T., Sjödin, P., Fredriksson, R., Boswell, T., Larsson, T. A., Salaneck, E., Zoorob, R., Mohell, N., and Larhammar, D. (2006) Neuropeptide Y-family receptors Y₆ and Y₇ in chicken. *FEBS J.* 273, 2048–2063.
- (6) Salaneck, E., Larsson, T. A., Larson, E. T., and Larhammar, D. (2008) Birth and death of neuropeptide Y receptor genes in relation to the teleost fish tetraploidization. *Gene* 409, 61–71.
- (7) Kanatani, A., Mashiko, S., Murai, N., Sugimoto, N., Ito, J., Fukuroda, T., Fukami, T., Morin, N., MacNeil, D. J., Van der Ploeg, L. H. T., Saga, Y., Nishimura, S., and Ihara, M. (2000) Role of the Y₁ receptor in the regulation of neuropeptide Y-mediated feeding: comparison of wild-type, Y₁ receptor-deficient, and Y₅ receptor-deficient mice. *Endocrinology* 141, 1011–1016.
- (8) Kanatani, A., Ishihara, A., Asahi, S., Tanaka, T., Ozaki, S., and Ihara, M. (1996) Potent neuropeptide Y Y₁ receptor antagonist, 1229U91: blockade of neuropeptide Y-induced and physiological food intake. *Endocrinology* 137, 3177–3182.

(9) Thiele, T. E., Koh, M. T., and Pedrazzini, T. (2002) Voluntary alcohol consumption is controlled via the neuropeptide Y Y₁ receptor. *J. Neurosci.* 22, RC208.

(10) Thorsell, A. (2007) Neuropeptide Y (NPY) in alcohol intake and dependence. *Peptides* 28, 480–483.

(11) Nilsson, T., Cantera, L., and Edvinsson, L. (1996) Presence of neuropeptide Y Y₁ receptor mediating vasoconstriction in human cerebral arteries. *Neurosci. Lett.* 204, 145–148.

(12) Edvinsson, L., Ekblad, E., Håkanson, R., and Wahlestedt, C. (1984) Neuropeptide Y potentiates the effect of various vasoconstrictor agents on rabbit blood vessels. *Br. J. Pharmacol.* 83, 519–525.

(13) Desai, S. J., Borkar, C. D., Nakhate, K. T., Subhedar, N. K., and Kokare, D. M. (2014) Neuropeptide Y attenuates anxiety- and depression-like effects of cholecystokinin-4 in mice. *Neuroscience* 277, 818–830.

(14) Wahlestedt, C., Pich, E. M., Koob, G. F., Yee, F., and Heilig, M. (1993) Modulation of anxiety and neuropeptide Y-Y₁ receptors by antisense oligodeoxynucleotides. *Science* 259, 528–531.

(15) Reubi, J., Gugger, M., and Waser, B. (2002) Co-expressed peptide receptors in breast cancer as a molecular basis for in vivo multireceptor tumour targeting. *Eur. J. Nucl. Med. Mol. Imaging* 29, 855–862.

(16) Körner, M., and Reubi, J. C. (2006) Chapter 62 - Somatostatin and NPY, in *Handbook of Biologically Active Peptides* (Abba, J. K., Ed.) pp 435–441, Academic Press, Burlington.

(17) Schneider, E., Mayer, M., Ziemek, R., Li, L., Hutzler, C., Bernhardt, G., and Buschauer, A. (2006) A simple and powerful flow cytometric method for the simultaneous determination of multiple parameters at G protein-coupled receptor subtypes. *ChemBioChem* 7, 1400–1409.

(18) Wieland, H. A., Engel, W., Eberlein, W., Rudolf, K., and Doods, H. N. (1998) Subtype selectivity of the novel nonpeptide neuropeptide Y Y₁ receptor antagonist BIBO 3304 and its effect on feeding in rodents. *Br. J. Pharmacol.* 125, 549–555.

(19) Schneider, E., Keller, M., Brennauer, A., Hoefelschweiger, B. K., Gross, D., Wolfbeis, O. S., Bernhardt, G., and Buschauer, A. (2007) Synthesis and characterization of the first fluorescent nonpeptide NPY Y₁ receptor antagonist. *ChemBioChem* 8, 1981–1988.

(20) Keller, M., Erdmann, D., Pop, N., Pluym, N., Teng, S., Bernhardt, G., and Buschauer, A. (2011) Red-fluorescent arginamide-type NPY Y₁ receptor antagonists as pharmacological tools. *Bioorg. Med. Chem.* 19, 2859–2878.

(21) Leban, J. J., Heyer, D., Landavazo, A., Matthews, J., Aulabaugh, A., and Daniels, A. J. (1995) Novel modified carboxy terminal fragments of neuropeptide Y with high affinity for Y₂-type receptors and potent functional antagonism at the Y₁-type receptor. *J. Med. Chem.* 38, 1150–1157.

(22) Guérin, B., Ait-Mohand, S., Tremblay, M.-C., Dumulon-Perreault, V. r., Fournier, P., and Bénard, F. (2010) Total solid-phase synthesis of NOTA-functionalized peptides for PET imaging. *Org. Lett.* 12, 280–283.

(23) Guérin, B., Dumulon-Perreault, V., Tremblay, M.-C., Ait-Mohand, S., Fournier, P., Dubuc, C., Authier, S., and Bénard, F. (2010) [Lys(DOTA)⁴]BVD15, a novel and potent neuropeptide Y analog designed for Y₁ receptor-targeted breast tumor imaging. *Bioorg. Med. Chem. Lett.* 20, 950–953.

(24) Liu, M., Mountford, S. J., Zhang, L., Lee, I.-C., Herzog, H., and Thompson, P. E. (2013) Synthesis of BVD15 peptide analogues as models for radioligands in tumour imaging. *Int. J. Pept. Res. Ther.* 19, 33–41.

(25) Northfield, S. E., Mountford, S. J., Wielens, J., Liu, M., Zhang, L., Herzog, H., Holliday, N. D., Scanlon, M. J., Parker, M. W., Chalmers, D. K., and Thompson, P. E. (2015) Propargyloxypoline regio- and stereoisomers for click-conjugation of peptide: synthesis and application in linear and cyclic peptides. *Aust. J. Chem.* 68, 1365.

(26) Zwanziger, D., Böhme, I., Lindner, D., and Beck-Sickingler, A. G. (2009) First selective agonist of the neuropeptide Y₁-receptor with reduced size. *J. Pept. Sci.* 15, 856–866.

(27) Nguyen, T., and Francis, M. B. (2003) Practical synthetic route to functionalized rhodamine dyes. *Org. Lett.* *5*, 3245–3248.

(28) Kilpatrick, L. E., Briddon, S. J., Hill, S. J., and Holliday, N. D. (2010) Quantitative analysis of neuropeptide Y receptor association with β -arrestin2 measured by bimolecular fluorescence complementation. *Br. J. Pharmacol.* *160*, 892–906.

(29) Mountford, S. J., Liu, M., Zhang, L., Groenen, M., Herzog, H., Holliday, N. D., and Thompson, P. E. (2014) Synthetic routes to the Neuropeptide Y Y₁ receptor antagonist 1229U91 and related analogues for SAR studies and cell-based imaging. *Org. Biomol. Chem.* *12*, 3271–3281.

(30) Holliday, N. D., Michel, M. C., and Cox, H. M. (2004) NPY receptor subtypes and their signal transduction, in *Neuropeptide Y and Related Peptides* (Michel, M. C., Ed.) pp 45–73, Springer, Berlin.

(31) Liu, M. J., Mountford, S. J., Zhang, L., Lee, I. C., Herzog, H., and Thompson, P. E. (2013) Synthesis of BVD15 peptide analogues as models for radioligands in tumour imaging. *Int. J. Pept. Res. Ther.* *19*, 33–41.

(32) Michel, M. C., Beck-Sickinger, A., Cox, H., Doods, H. N., Herzog, H., Larhammar, D., Quirion, R., Schwartz, T., and Westfall, T. (1998) XVI. International Union of Pharmacology recommendations for the nomenclature of neuropeptide Y, peptide YY, and pancreatic polypeptide receptors. *Pharmacol. Rev.* *50*, 143–50.

(33) Stott, L. A., Hall, D. A., and Holliday, N. D. (2016) Unravelling intrinsic efficacy and ligand bias at G protein coupled receptors: A practical guide to assessing functional data. *Biochem. Pharmacol.* *101*, 1–12.

(34) Parker, E. M., Babij, C. K., Balasubramaniam, A., Burrier, R. E., Guzzi, M., Hamud, F., Gitali, M., Rudinski, M. S., Tao, Z., Tice, M., Xia, L., Mullins, D. E., and Salisbury, B. G. (1998) GR231118 (1229U91) and other analogues of the C-terminus of neuropeptide Y are potent neuropeptide Y Y₁ receptor antagonists and neuropeptide Y Y₄ receptor agonists. *Eur. J. Pharmacol.* *349*, 97–105.

(35) Balasubramaniam, A., Dhawan, V. C., Mullins, D. E., Chance, W. T., Sheriff, S., Guzzi, M., Prabhakaran, M., and Parker, E. M. (2001) Highly selective and potent neuropeptide Y (NPY) Y₁ receptor antagonists based on [Pro(30), Tyr(32), Leu(34)]NPY(28–36)-NH₂ (BW1911U90). *J. Med. Chem.* *44*, 1479–1482.

(36) Liu, M., Mountford, S. J., Richardson, R. R., Groenen, M., Holliday, N. D., and Thompson, P. E. (2016) Optically Pure, Structural, and Fluorescent Analogues of a Dimeric Y₄ Receptor Agonist Derived by an Olefin Metathesis Approach. *J. Med. Chem.* *59*, 6059–6069.

(37) Kuhn, K. K., Ertl, T., Dukorn, S., Keller, M., Bernhardt, G., Reiser, O., and Buschauer, A. (2016) High Affinity Agonists of the Neuropeptide Y (NPY) Y₄ Receptor Derived from the C-Terminal Pentapeptide of Human Pancreatic Polypeptide (hPP): Synthesis, Stereochemical Discrimination, and Radiolabeling. *J. Med. Chem.* *59*, 6045–6058.

(38) Kilpatrick, L. E., Briddon, S. J., and Holliday, N. D. (2012) Fluorescence correlation spectroscopy, combined with bimolecular fluorescence complementation, reveals the effects of β -arrestin complexes and endocytic targeting on the membrane mobility of neuropeptide Y receptors. *Biochim. Biophys. Acta, Mol. Cell Res.* *1823*, 1068–1081.